UNIVERSITY OF CALIFORNIA

Los Angeles

Sequential Stroke Model of Vascular Dementia

A thesis submitted in partial satisfaction of the

requirements for the degree of

Master of Science in Physiological Science

by

Mary Hovanesyan

2024

ABSTRACT OF THE THESIS

Sequential Stroke Model of Vascular Dementia

by

Mary Hovanesyan

Master of Science in Physiological Science

University of California, Los Angeles, 2024

Professor Patricia Emory Phelps, Co-Chair

Professor Stanley Thomas Carmichael, Co-Chair

White matter stroke (WMS) is a debilitating disorder, characterized by the formation of ischemic lesions along the white matter tracts in the brain. The accumulation of these white matter lesions leads to vascular dementia, which is the second leading cause of dementia, and accelerates the pathology of Alzheimer's Disease [11]. Currently, there are no therapy options available to halt the progression of vascular dementia. Hence, we wanted to better understand the molecular mechanisms and behavioral outcomes that may result as a consequence of multiple strokes happening within the white matter region of the brain. We created a two-stroke protocol in which an initial large white matter stroke was induced in C57BL/6J mice models, then 1-month later, a small white matter stroke was induced contralaterally. This models the progressive nature of ischemic white matter damage, which is a core feature of the human condition. We measured the recovery of these cohorts through motor behavior tests (grid-walking and pole test) and cognitive tests (fear conditioning and novel object recognition) at baseline, 1-month, 2-month, and 3-month timepoints. Our data indicates that for the grid-walking test, the Large WMS mice have significantly more foot faults at the 1-month and 2-month timepoints, and then

plateau at the 3-month timepoint, when compared to the Large WMS + Small WMS. In the pole test at the 3-month timepoint, the Large WMS mice have shorter t-turn times when compared to the Large WMS + Small WMS cohort. During the fear conditioning test, the Large WMS mice had higher freeze times across all timepoints when compared to the Large WMS + Small WMS mice. Overall, this data suggests that the Large WMS + Small WMS mice have more difficulty performing fine motor tasks, such as the pole test, at a later timepoint and have hindered memory and recall ability when compared to the Large WMS only cohort.

The thesis of Mary Hovanesyan is approved.

Amy Catherine Rowat

Patricia Emory Phelps, Committee Co-Chair

Stanley Thomas Carmichael, Committee Co-Chair

University of California, Los Angeles

2024

Table of Contents

List of Figures

Acknowledgments

My time in the Carmichael lab has been pivotal for my academic career and professional development. I would like to thank my mentor, Dr. Carmichael, for his unwavering support and scientific guidance. He has made me a better researcher and has constantly challenged me to think outside the box. I would also like to thank all the members of the Carmichael lab, past and present, for their advice during times of need. I'm eternally grateful for all the support they have given me, and for being great resources during my time in the lab. Lastly, I would like to thank my thesis committee for their guidance during my graduate training. I have enjoyed my time at UCLA, and am excited for my future endeavors.

Introduction

Every year in the United States, there are around 795,000 individuals that experience the debilitating impacts of having a stroke [3]. Of those 795,000 individuals, 610,000 are first time strokes and the remaining 185,000 are individuals that experience a sequential stroke within a 5-year timeframe [3]. Unfortunately, at this time, there are no current therapy options available that will provide patients with a full recovery. Individuals may find themselves working with speech, physical, and occupational therapists after having a stroke in order to regain motor and cognitive function [19]. While progress can be made through these therapies, some patients are left with permanent limitations post-stroke. Therefore, researchers have tried to better understand the molecular and behavioral changes that occur after an injury in order to develop permanent treatments for these individuals, based on the type of stroke they have undergone.

There are around five different types of strokes that individuals may have: ischemic, transient ischemic attack (mini-stroke), cryptogenic stroke, brain stem stroke, and hemorrhagic stroke [6]. Out of the five, ischemic and hemorrhagic are the two most common types of strokes, with ischemic being the most prevalent [6]. Approximately, 8 out of 10 strokes that occur are categorized as ischemic strokes [6]. An ischemic stroke is a result of a blood clot that forms within the brain due to plaque buildup within the inner linings of the blood vessel [6]. A hemorrhagic stroke on the other hand is due to bleeding in the brain caused by a ruptured blood vessel [20]. With the large population of individuals suffering from an ischemic stroke, researchers have concentrated on finding treatments for this type of stroke. By understanding and investigating the differences in gray matter versus white matter damage, researchers can accurately diagnose and treat individuals properly based on the region where the injury occurred.

Gray and white matter are two essential components that make up our brain and spinal cord [8,10,12]. Gray matter is composed mostly of neuronal cell bodies, axon terminals, dendrites, and nerve synapses, and is the area where most of our information processing occurs [8,10,12]. We process sensation, perception, voluntary movement, learning, speech, and cognition within the gray matter [8,10,12]. On the other hand, white matter is made up of mostly axons which help with signal transmission of electrical impulses from one region of the brain and spinal cord to another [8,10,12]. Our brain is composed of approximately 40% gray matter and 60% white matter [8,10,12]. With such a large composition of white matter, researchers have looked to better understand what happens to individuals when injury is present within this area.

Diseases that occur within the gray matter are primarily composed of neurodegenerative diseases like Alzheimer's disease, Parkinson's disease, and even stroke [10,12]. Although changes within the white matter may occur in these diseases, the major physiological changes occur within the gray matter region [8]. On the other hand, white matter diseases are often associated with illnesses like multiple sclerosis, spinal cord injury, and stroke [8]. Although diseases like stroke can occur within both the gray and white matter, the white matter is more vulnerable to ischemia and is often more severely injured than gray matter [22].

White matter ischemia comprises up to 30% of all strokes, with many events going undiagnosed in the early stages of disease onset [2,22]. These infarcts produce cognitive impairments with motor and sensory loss [2,22]. Ischemic lesions can be detected clinically in patients by using MRI imaging techniques to visualize hyperintensities within the white matter [22]. The cells primarily affected in the brain after a white matter stroke (WMS) include: astrocytes, axons, oligodendrocytes, and myelin [2]. Over time, it has been found that a WMS

expands into adjacent white matter producing large lesions over time, increasing the difficulties that later present as vascular dementia [2].

Recent research has found that 25-30% of ischemic stroke survivors develop immediate or delayed vascular cognitive impairment (VCI) or vascular dementia (VaD) [5]. Vascular dementia (VaD) is the second most common form of dementia after Alzheimer's disease [4,11]. VaD occurs when the blood supply to regions of the brain becomes reduced due to an occlusion in the blood vessel, a stroke, or a series of small strokes [4,11]. Some symptoms for patients with VaD might include confusion, trouble concentrating, problems with memory, and unsteady gait [11]. These symptoms may develop gradually or become apparent after stroke [4]. There are two main types of vascular dementia that occur, mixed dementia or multi-infarct dementia [4]. Mixed dementia occurs when individuals experience symptoms of both vascular dementia and Alzheimer's disease [4]. Multi-infarct dementia occurs from repeated small 'silent' blockades [4]. These blockades might not be apparent at first, but over time, can cause symptoms of impairment and lead to vascular cognitive impairment [4].

White matter and gray matter injuries also differ in the cell types that are injured and the tissue environments that they form. Gray matter is the site of neuronal cell bodies, their dendrites and synaptic connections [10,12]. This neuronal synaptic network and structure dominates the cellular architecture in gray matter diseases. For example, neurodegenerative diseases such as Alzheimer's disease affect synaptic connections on neurons. On the other hand, the white matter is an area devoid of neuronal cell bodies, but categorized with a large-scale presence of neuronal connections, dendrites and their synapses [21]. The white matter contains glial cells and vascular support structures. This cellular system is termed the white matter neurovascular niche:

oligodendrocytes, oligodendrocyte precursor cells (OPCs), astrocytes (these three are the glial cells of white matter), endothelial cells, pericytes and microglia [21]. Each of these cells' contacts with, and signals to, each other. White matter diseases occur when these cells are damaged. The axons that run between the brain areas are carried in white matter and often myelinated by oligodendrocytes. These axonal connections may be injured when the glial cells are injured. In studies of tissue outcomes and progression in diseases such as white matter stroke or vascular dementia, these cells of the neurovascular niche are a primary focus.

Researchers have further investigated and developed white matter stroke models using rodents to better understand white matter ischemia. In recent studies, scientists have induced white matter injury in these models by doing carotid artery stenosis using external micro-coils [10,17]. White matter lesions are induced within the corpus callosum, anterior commissure, and optic nerve [10,17]. While there are no obvious involvements in the gray matter using this method, the histological features of these lesions have not been properly characterized, posing some limitations of this method [10,17]. An alternative approach to induce white matter injury is by doing a local stereotaxic injection of a vasoconstrictive agent called endothelin-1 [9,17]. Endothelin-1 is used to reduce blood flow, and induce focal ischemic lesions without disrupting the blood brain barrier [9,17]. This model causes axonal injury and disruption to myelin, however, this method also has its limitations as well, as the induction of an inflammatory response isn't necessarily observed in humans.

While both these models have provided researchers insight into white matter ischemia, no current models have been developed to investigate the multitude of cases that VaD patients experience. VaD patients have multiple ischemic lesions within the white matter region of their brain, which accelerates the onset of Alzheimer's disease and presents an urgent need to better

understand this disease in the clinic. In order to investigate this, we created a sequential stroke model of vascular dementia to better understand the cellular damage that occurs within the white matter region, and have conducted several behavioral and cognitive tests to investigate the impairments that are present after injury.

Materials and Methods

Mice. 10-week-old C57BL/6J (Jackson Laboratories) mice were used in this study. There was a total of 45 mice (15 mice/group) for motor behavior tests and 36 mice (12 mice/group) for cognitive behavior tests. All mice were housed in a temperature-controlled vivarium that ran on a 12-h light/dark cycle. All experiments were performed in accordance with the National Institute of Health animal protection guidelines and were approved by the University of California, Los Angeles Chancellor's Animal Research Committee.

Large White Matter Stroke. A large white matter stroke [7,13,16] was induced in the left hemisphere of 10-week-old male C57BL/6J mice (Jackson Laboratories). For this model, three (300nl) injections of a vasoconstrictor N5-(1-iminoethyl)-L-ornithine (L-NIO; 27mg/ml in sterile physiological saline; Millipore) were made into the white matter region of the brain, leading to focal ischemia (Figure 1A). The three injections were made at the following coordinates: anterior-posterior (AP) 0.35, medio-lateral (ML) 2.00, dorsoventral (DV) -1.40; AP 0.35, ML 3.00, DV -1.45; AP 0.35, ML 3.66, DV -1.50. The L-Nio was injected using a Nanoliter 2020 Injector (World Precision Instruments) via a micropipette that was positioned at a 36° angle to avoid damage to the cortex. The micropipette was left *in situ* for 10 minutes post-injection to allow proper diffusion. The mice were anesthetized with 2% isoflurane onto a stereotaxic apparatus and core body temperature was maintained at 37 ± 0.5 °C (RightTempTM, Kent Scientific, Torrington, CT).

Sequential Small White Matter Stroke. A small white matter stroke was induced in the right hemisphere of the brain 1-month after the large white matter stroke was induced (Figure 1B). For this model, one focal (300nl) microinjection of a vasoconstrictor N5-(1-iminoethyl)-L-ornithine (L-NIO) was injected into male C57BL/6J mice (Jackson Laboratories). The coordinates for the injection were anterior-posterior (AP) 0.65, medio-lateral (ML) 1.20, and dorsoventral (DV) -1.46. The L-Nio was injected via a micropipette at a 90° angle using a Nanoliter 2020 Injector (World Precision Instruments). The micropipette was left *in situ* for 10 minutes post-injection to allow proper diffusion. The mice were anesthetized with 2% isoflurane onto a stereotaxic apparatus and core body temperature was maintained at 37 ± 0.5 °C (RightTempTM, Kent Scientific, Torrington, CT).

Motor Behavior Tests

Grid-walking. We conducted a grid-walking test to assess innate motor control. The protocol was conducted as described with slight modifications [18]. The researcher was blinded to the different conditions and cohorts when conducting the test and analyzing all the grid-walking videos. Mice were individually placed on a mesh wire grid (1.5cm x 1.5cm squares) for 5 minutes. Each 5-minute session was video recorded, and the number of right forelimb footfalls were counted within the first 50 steps. Cohorts were tested at the following timepoints: baseline, 1-month, 2-month, and 3-months post-stroke.

Pole Test. To assess motor coordination, we conducted a pole test at the 3-month timepoint as described [14] with slight modifications. The researcher was blinded to the different conditions and cohorts when conducting the test and analyzing all the pole test videos. For this test, mice

were individually placed facing upward on top of a wooden pole (9.5mm diameter, and 50cm long). The time it took for each mouse to turn around and climb down to the bottom of the pole (t-turn) was recorded. Each mouse had 60 seconds to reach the bottom of the pole for each trial. There was a total of 5 consecutive trials per mouse, with all trials being conducted on the same day. If the mouse failed to turn around the pole within the 60 seconds, or fell off of the pole once placed on it, a maximum of 60 seconds was recorded for that trial. The timer was stopped once the head of the mouse reached the base of the pole.

Cognitive Behavioral Tests

Novel Object Recognition. To assess recognition memory, mice were tested for novel object recognition [1] as described with slight modifications. The test was conducted at two timepoints: baseline and 3-months post-stroke. The researcher was blinded to the different conditions and cohorts when conducting the test and analyzing the data. During the habituation phase, mice were placed individually in open field chambers, and were allowed to explore the environment for 30 minutes. Following the habituation phase, an acquisition phase was conducted in which the mice were returned to the open field chambers with two identical objects placed in opposite corners, and were allowed to explore both items for 10 minutes. On test day, the mice were returned to the same open field chambers for 10 minutes, and were exposed to 1 familiar object and 1 novel object. A discrimination index was used to assess preference of the novel object to the familiar object.

Fear Conditioning. To assess aversive memory, mice were tested for fear conditioning [15] as described with slight modifications. The mice were tested at various time points: baseline, 1-month, 2-month, and 3-months post-stroke. The researcher was blinded to the different

conditions and cohorts when conducting the test and analyzing the data. During the training, mice were allowed to be acclimated to the room for 1 hour, then were placed on a shock grid (shocked 3 times at 0.75mAmp, with a 2 second shock inter-trial interval of 1 minute). Twenty-four hours after the training, the mice were tested by being returned to the training context for 4 minutes, and were assessed for their memory of the training event. This 4-minute test was conducted at the four time points (baseline, 1-month, 2-month, and 3-months) following a stroke.

Immunohistochemistry. Animals were transcardially perfused with 0.1M phosphate-buffered saline (PBS), followed by 4% paraformaldehyde (PFA). The brains were removed, postfixed overnight in 4% PFA, cryoprotected for 2 days in 30% sucrose, and frozen in -80°C. The tissue was sectioned into parallel series of 35 µm thick sections 245 µm apart (Leica CM 3050). An antigen retrieval protocol was used for immunohistochemistry staining. The sections were incubated in sodium citrate at 80°C for 20 minutes, followed by 10-minutes at room temperature in sodium citrate. The sections were later incubated in a blocking solution containing 5% normal donkey serum for 1 hour at room temperature, and left in primary antibodies for two days overnight at 4°C. The primary antibodies used were NF160 (1:500, Abcam, cat #ab7794), MBP (1:500, Abcam, cat #ab7349), and GFAP (1:500, Abcam, cat #ab4674). On the third day, the sections were incubated with fluorescence dye-conjugated secondary antibodies (Jackson ImmunoResearch) for 1 hour at room temperature.

Image Analysis

Ventricle Volume Measurement. Brain sections were stained with NF160, MBP, and GFAP antibodies. Full section images were taken using an Epifluorescence microscope (20x objective; Nikon). The ventricles were outlined using the polygon tool in the ImageJ software. Ventricle

volume was calculated by first converting the area (given in pixels) to millimeters squared. The area (mm^2) was multiplied by the section thickness (0.035mm) to get the ventricle volume for each section.

White Matter Volume Measurement. Brain sections were stained with NF160, MBP, and GFAP antibodies. Full section images were taken using an Epifluorescence microscope (20x objective; Nikon). Using the ImageJ software, the white matter for each section was outlined using the polygon tool. The area (given in pixels) was then converted to millimeters squared. The area (mm^2) was multiplied by the section thickness (0.035mm) to get the white matter volume.

Quantification of NF160, MBP, and GFAP Intensity in White Matter. Five sections per cohort were analyzed for NF160, MBP, and GFAP using an immunohistochemistry protocol. Full section images were taken for each condition using an Epifluorescence microscope (20x objective; Nikon). Images were loaded into the ImageJ software, and channels were separated. The white matter was outlined for each section using the polygon tool. The area (given in pixels) was converted to millimeters squared. The area (mm^2) was then multiplied with the mean value (quantified by ImageJ) to get the intensity of each antibody.

Statistical Analysis. All data was reported as a mean with standard error mean (SEM). Statistical analysis for motor and cognitive behavior, except the pole test, was analyzed using GraphPad Prism. For both grid-walking and novel object recognition tests, a mixed effects analysis was conducted via Tukey's multiple comparisons test. The pole test was analyzed using a logistic mixed effects regression model via RStudio. Fear conditioning tests were analyzed using mixed effects analysis by doing a Dunnett's multiple comparisons test. All image analysis was done through ImageJ. Ventricle volume, white matter volume, and NF160/MBP/GFAP

intensity in the white matter was analyzed via GraphPad Prism using two-way ANOVA and Tukey's multiple comparisons test.

Results

Motor Behavior Tests

Large WMS mice display higher foot faults in grid-walking test. A grid-walking test was used to assess innate motor control at four different timepoints: baseline, 1- month, 2-month, and 3-months post-stroke. Compared to the Control, the Large WMS mice displayed significantly more foot faults at the 1-month and 2-month timepoints (Figure 2). Foot faults plateaued at the 3-month timepoint for the Large WMS cohort, and reached similar levels to the Large WMS + Small WMS cohort (Figure 2). These results indicate that mice with single strokes have more difficulty in performing innate motor tasks such as grid-walking when compared to a sequential white matter stroke model.

Large WMS + Small WMS mice have higher t-turn times in pole test. A pole test was conducted at the 3-month timepoint to assess motor coordination among cohorts. The Large WMS + Small WMS mice had higher turn times in the first, second, fourth and fifth trials (Figure 3). Overall, it seems that the two-stroke model hinders the ability of the mice to have controlled movement down the pole, resulting in the Large WMS + Small WMS mice to have longer turn times going down the pole versus the Large WMS and Control mice.

Cognitive Tests

Large WMS mice display higher recall and memory in fear conditioning test. To assess learning and memory, a fear conditioning test was conducted at baseline, 1-month, 2-month, and 3-month timepoints. Across all timepoints, the Large WMS cohort had higher freeze times when compared to the Control and Large WMS + Small WMS cohorts (Figure 4). Significant differences were found at the 2-month timepoint between the Control and Large WMS cohorts.

This data indicates that a sequential stroke model greatly hinders the ability of mice to recall information when compared to the single stroke mice.

No display of memory in novel object recognition test among all three cohorts. Mice were assessed for recognition memory in the novel object recognition test at two timepoints: baseline and 3-months post stroke. Among the three cohorts, no differences were found at either timepoints (Figure 5). At the 3-month timepoint, very few animals from the Large WMS and Large WMS + Small WMS cohorts seemed to recall the familiar object, and instead spent more time exploring the novel object at the 3-month timepoint (Figure 5). There was experimental error in conducting the novel object recognition test, as the fear conditioning test was conducted right before, thus interfering with the mice learning and memory. Next time when conducting the novel object recognition test, we will make sure to do these set of experiments prior to the fear conditioning test to avoid the association of fear within the context of the novel object recognition test.

Tissue Analysis

Differences in ventricle volume among all three cohorts.

The ventricle volume was measured among each cohort to assess damage caused by the white matter stroke. All imaging was done at the 3-month timepoint. On the ipsilateral side to the Large WMS, the ventricle volume was significantly larger in the Large WMS cohort when compared to the Control (Figure 6B). However, on the contralateral side to the Large WMS, no significant differences were seen between the three cohorts (Figure 6B). These results suggest that several mechanisms such as tissue loss might be an indication of enlarged ventricle volume within the Large WMS cohort on the ipsilateral side to the stroke.

White matter volume is thinner in both stroke cohorts compared to Control. White matter volume was measured among all three cohorts to assess tissue damage after a white matter stroke. All imaging was done at the 3-month timepoint. On the ipsilateral side to the Large WMS, the white matter was significantly thinner in the Large WMS and Large WMS + Small WMS cohorts when compared to the Control (Figure 7B). On the contralateral side to the Large WMS, the white matter volume was also significantly less in both the Large WMS and Large WMS + Small WMS cohorts when compared to the Control (Figure 7B). This data indicates that there is significant white matter loss following a stroke in both Large WMS and Large WMS + Small WMS cohorts when compared to the Control on both the ipsilateral and contralateral sides.

Lower NF160 intensity in white matter region of both stroke cohorts when compared to Control. NF160 intensity was measured to assess axonal loss after a white matter stroke. All imaging was done at the 3-month timepoint. On the ipsilateral side to the Large WMS, there was significantly less NF160 intensity in both the Large WMS and Large WMS + Small WMS cohorts when compared to the Control (Figure 8B). On the contralateral side to the Large WMS, the NF160 intensity was also significantly less in the Large WMS and Large WMS + Small WMS cohorts when compared to the Control (Figure 8B). This data indicates that following a white matter stroke, axons are significantly depleted within the white matter region of the brain.

Less MBP intensity in the white matter region of both stroke cohorts when compared to Control. MBP intensity was measured within the white matter to assess myelin loss following a white matter stroke. All imaging was done at the 3-month timepoint. When looking at the ipsilateral to the Large WMS, both the Large WMS and Large WMS + Small WMS cohorts had significantly less MBP intensity within the white matter region when compared to the Control (Figure 9B). The MBP intensity levels on the contralateral side to the Large WMS were also

significantly less in the stroke cohorts when compared to the Control (Figure 9B). These results indicate that the myelin is significantly depleted within the white matter of the Large WMS and Large WMS + Small WMS cohorts when compared to the Control in both the ipsilateral and contralateral sides to the Large WMS.

Less GFAP Intensity in the white matter region of both stroke cohorts when compared to Control. The GFAP intensity was measured within the white matter region to assess the presence of reactive astrocytes following a white matter stroke. All imaging was done at the 3-month timepoint. On the ipsilateral to Large WMS position, there was significantly less GFAP intensity in the white matter for both the Large WMS and Large WMS + Small WMS cohorts when compared to the Control (Figure 10B). On the contralateral side to Large WMS position, there were differences present in the GFAP levels among the three cohorts. The single stroke model had significantly less GFAP levels when compared to the Control on the contralateral side to the Large WMS (Figure 10B). The sequential small white matter stroke model had higher levels of GFAP in both the ipsilateral and contralateral sides when compared to the Large WMS, but was still less than Control. These results may indicate that a double stroke induces more astrocyte reactivity in both hemispheres when compared to a single stroke.

Discussion

In the present study, we were interested in investigating how mice that had received a sequential stroke would differ in their behavioral and cognitive tasks, as well as histological differences, compared to the other two cohorts. With the motor behavior and cognitive tests, we saw that the sequential stroke mice performed slower in the fine motor tasks, such as the pole test. The Large WMS + Small WMS mice were also not able to recall information as well as the single stroke mice in the fear conditioning test. The histological differences among the three cohorts differed, with there being variations in the ipsilateral and contralateral side to the Large WMS. Overall, the sequential stroke model had low levels of NF160, MBP, and GFAP in the white matter when compared to Control.

The results from the motor tests may suggest that in tasks such as grid-walking that assess innate motor control, the sequential stroke may not have as big of an effect as the single stroke mice. The single Large WMS seems to hinder the ability of the mice to control their movement much more than the sequential stroke mice. Contrarily, when looking at the pole test, we saw that the Large WMS + Small WMS had a significant negative effect on the ability of the mice to control their movement. This may suggest that when challenged to accomplish tasks that utilize fine motor movement, mice have substantially more difficulty completing the task when induced with two strokes. These results may translate to humans, and provide researchers and physicians with data on how they can personalize treatments and therapies to differ for individuals with single strokes versus sequential strokes. Patients may be completing these motor tasks at different rates due to the number of strokes they had within the white matter region of the brain.

With the cognitive tests, we saw that the sequential stroke mice were not able to recall information as well as the single stroke mice or Control. The histological results showed that the single stroke mice had low levels of NF160, MBP, and GFAP in both the ipsilateral and contralateral positions when compared to Control. However, when looking at the NF160, MBP, and GFAP levels of the sequential stroke mice, they seemed to have higher levels of all three stains in both the ipsilateral and contralateral positions when compared to the Large WMS. These results may suggest that there may be a recovery process being activated within the white matter region soon after a second stroke has been induced. Prior literature states that there may be a neuroprotective effect being induced by the second stroke [24]. The sequential white matter stroke may be re-activating the repair process, inducing recovery from the first stroke [24].

While prior literature has given us insight into the neuroprotective abilities of a two-stroke model, it lacks in investigating what would happen if each stroke were to be induced in opposite hemispheres. Researchers have only investigated a two-stroke model in the cortex, ipsilateral to each other [24]. However, this doesn't mimic the pathology we would see in patients with vascular dementia. Therefore, it was crucial that we created a sequential white matter stroke model, and investigated the potential recovery effects that were induced by the second stroke. These findings can help researchers and physicians better understand the limitations present in patients with vascular dementia, and how we can speed up the recovery process.

In future experimentation, we want to conduct the pole test at earlier timepoints to see how the motor deficits are different among the three cohorts. Additionally, we want to conduct the novel object recognition at a few more timepoints in between baseline and 3-months. Overall, the novel object recognition test will be conducted prior to the fear conditioning test to not hinder

the results of memory recall. The results from these experiments may encourage us to try this model in aged mice, as individuals who have vascular dementia tend to fall in this demographic.

Figures

Figure 1: Large White Matter Stroke & Sequential Small White Matter Stroke Models

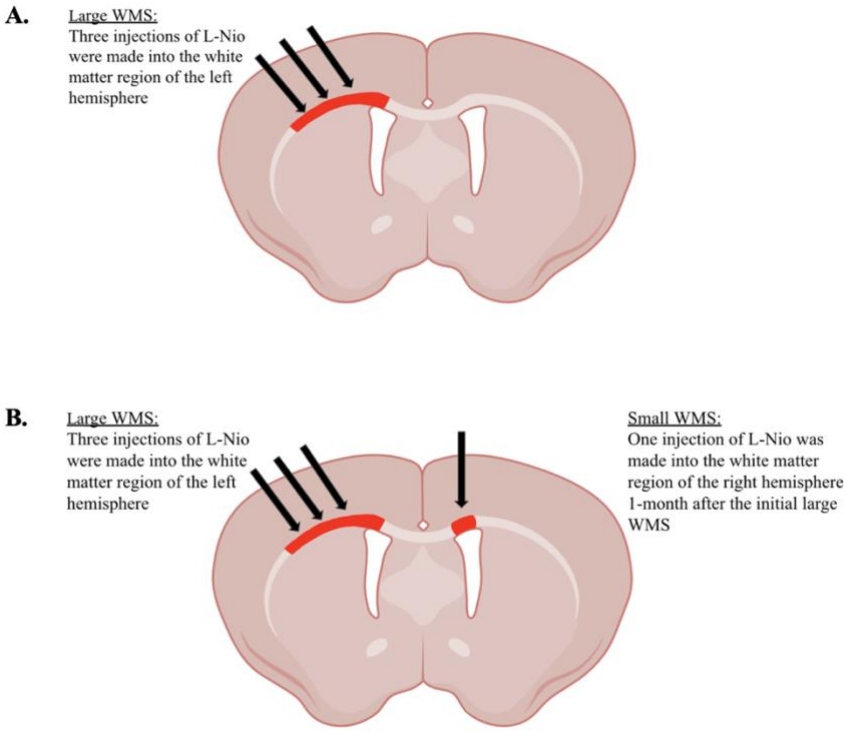

Figure 1: (A) A large white matter stroke was initially induced into the white matter region of the left hemisphere of the brain. (B) One month after the induction of the large white matter stroke, a sequential small white matter stroke was induced within the white matter of the contralateral hemisphere.

Figure 2: Large White Matter Stroke (WMS) mice show deficit in grid-walking test at 1-month and 2-month timepoints when compared to Control.

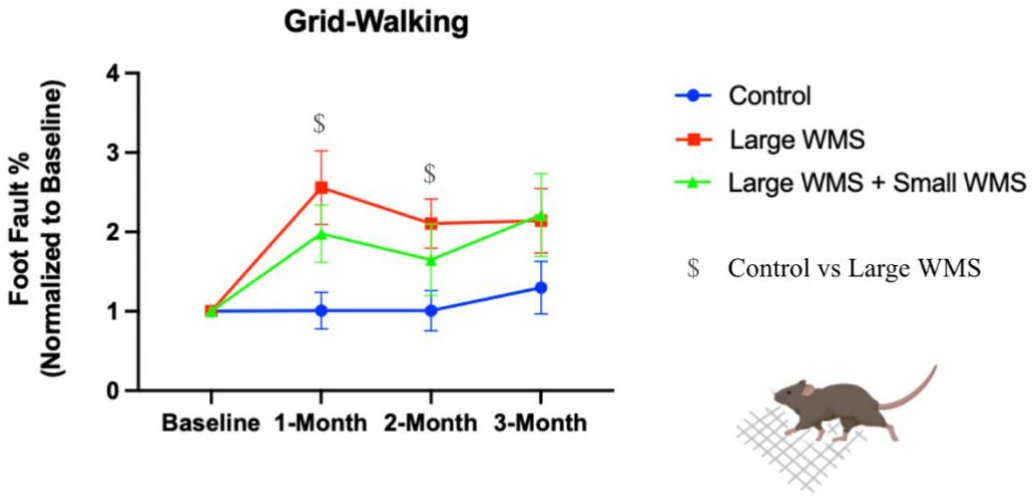

Figure 2: Grid-walking test. n=15 mice per group for Control and Large + Small WMS at all timepoints; n=14 mice for Large WMS at the 3-month timepoint; $P<0.05: Control vs Large WMS, mixed effects analysis was conducted via Tukey's multiple comparisons test; values are mean with standard error mean (SEM).

Figure 3: Large WMS + Small WMS mice have significantly higher t-turn times in the fourth and fifth trials when compared to Control and Large WMS cohorts.

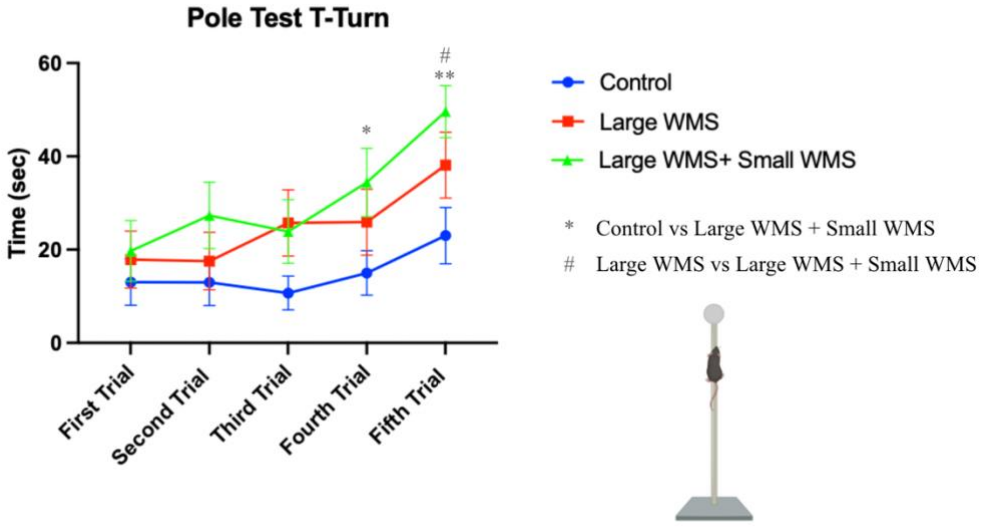

Figure 3: Pole test. Mice were placed facing upwards on a wooden pole near the top. All five trials for each mouse were conducted on the same day. Large WMS + Small WMS mice took longer in the fourth and fifth trials and were unable to get down the pole, displaying impairments in motor control due to a sequential stroke. n= 15 for Control and Large WMS + Small WMS cohorts; n=14 for Large WMS cohort; *P< 0.05: Control vs Large WMS + Small WMS, **P<0.01: Control vs Large WMS + Small WMS, #P<0.05: Large WMS vs Large WMS + Small WMS, graph reported as mean with standard error mean (SEM), statistical analysis conducted using logistic mixed effects regression model via RStudio.

Figure 4: In the Fear Conditioning Test, Large WMS mice have significantly higher freeze times at the 2-month timepoint when compared to Control and Large WMS + Small WMS cohorts.

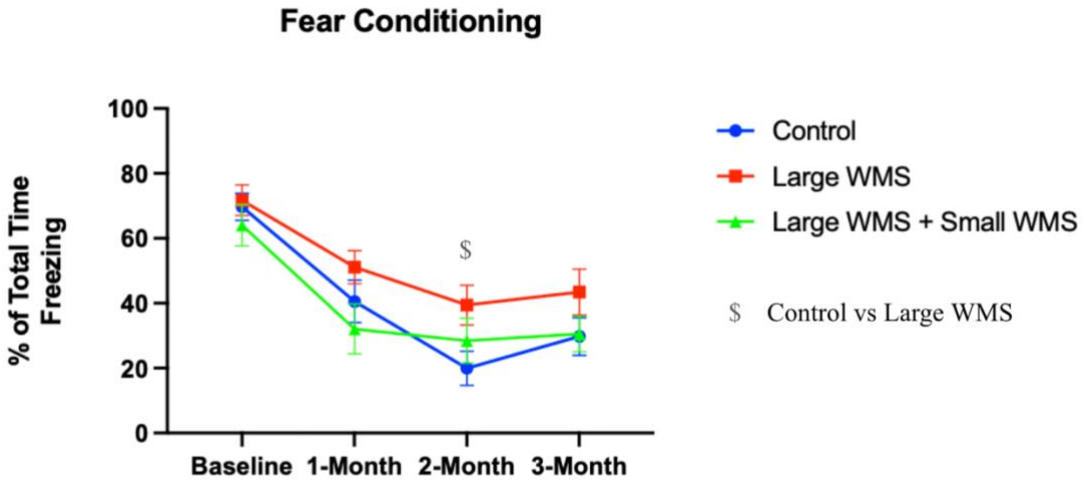

Figure 4: Fear conditioning test. n=12 for Control at all timepoints; n=12 for Large WMS at baseline and n=11 for Large WMS at 1-month, 2-month, and 3-month timepoints; n=11 for Large WMS + Small WMS at all timepoints; $P< 0.05: Control vs Large WMS, mixed effects analysis was conducted via Dunnett's multiple comparisons test; values are mean with standard error mean (SEM).

Figure 5: In the Novel Object Test, there were no significant differences between the cohorts at baseline and 3-month timepoints.

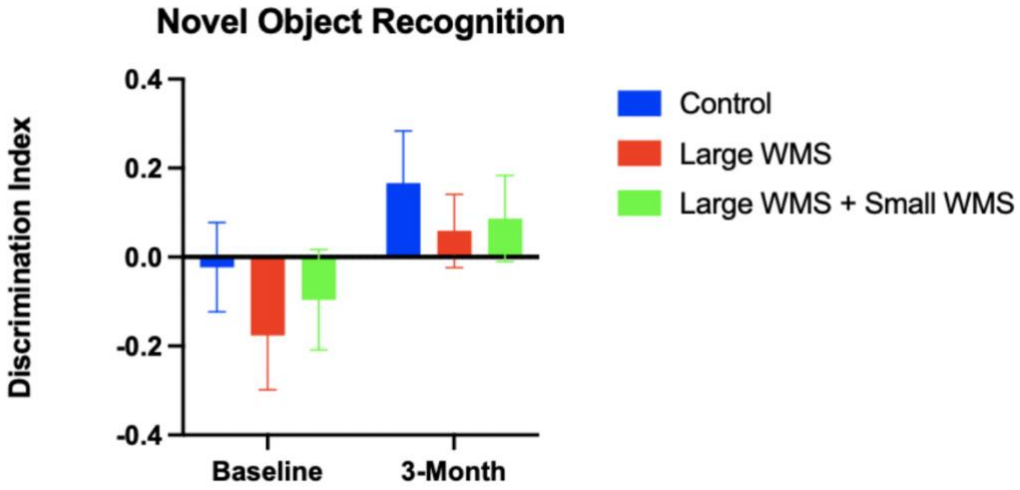

Figure 5: Novel Object Recognition test. n= 12 for Control and Large WMS + Small WMS at baseline and 3-months post stroke; n=12 for Large WMS at baseline and n=11 for Large WMS at the 3-month timepoint; mixed effects analysis was conducted via Tukey's multiple comparisons test; values are mean with standard error mean (SEM).

Figure 6: Significantly larger ventricle volume in the Large WMS cohort on the ipsilateral side when compared to Control.

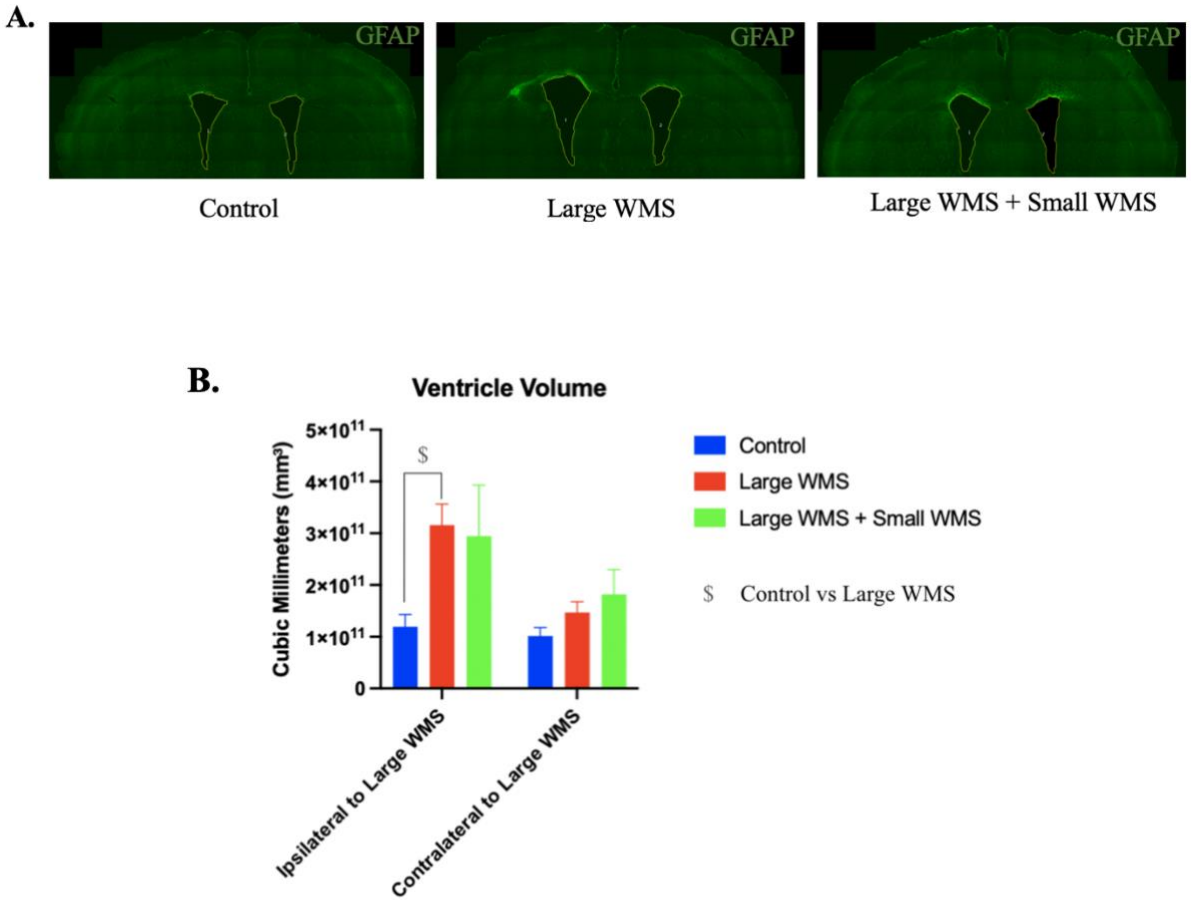

Figure 6: **(A)** Ventricle volume quantification for each cohort was analyzed separately using tissue sections that were processed for GFAP immunoreactivity. **(B)** Quantification of ventricle volume. n= 5; $P< 0.05: Control vs Large WMS, Two-way ANOVA was conducted via Tukey's multiple comparisons test; values are mean with standard error mean (SEM).

Figure 7: Less white matter volume in Large WMS and Large WMS + Small WMS cohorts when compared to Control.

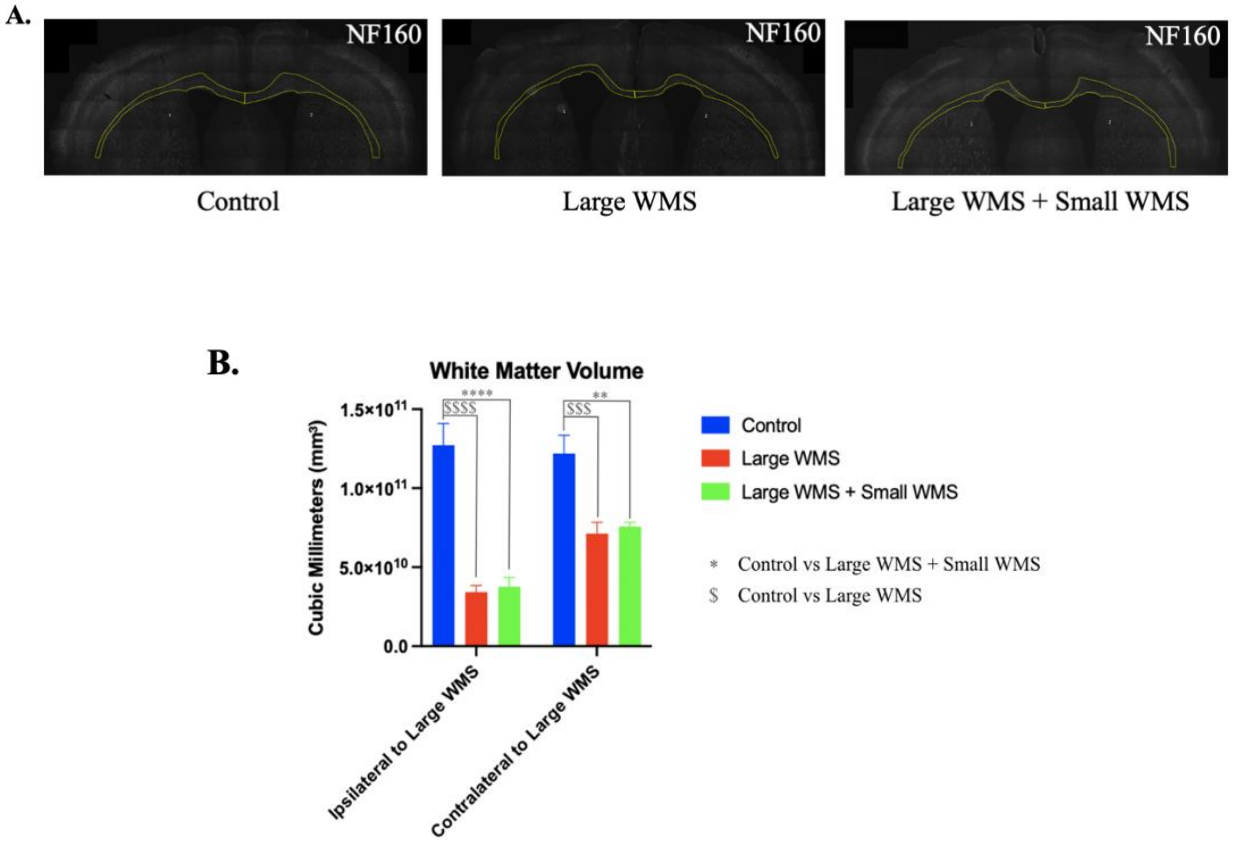

Figure 7: **(A)** All tissue sections were from the 3-month timepoint. Each section was analyzed separately for white matter volume quantification using samples stained with NF160. **(B)** Quantification of white matter volume. n= 5; **P<0.01: Control vs Large WMS + Small WMS, ****P<0.0001: Control vs Large WMS + Small WMS, $$$ P<0.001: Control vs Large WMS, $$$$P<0.0001: Control vs Large WMS, Two-way ANOVA was conducted via Tukey's multiple comparisons test; values are mean with standard error mean (SEM).

Figure 8: Less NF160 intensity in the white matter of Large WMS and Large WMS + Small WMS cohorts.

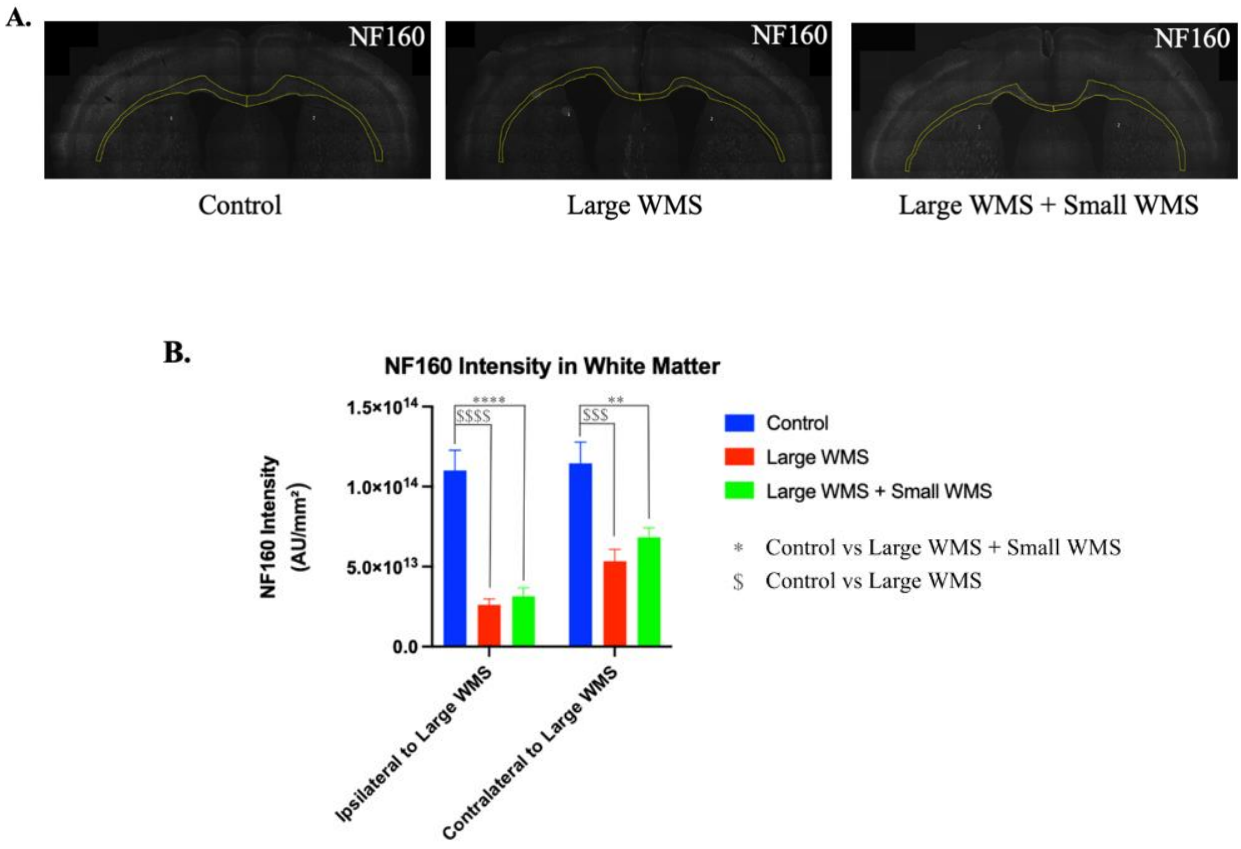

Figure 8: **(A)** Sections were stained with NF160 for intensity quantification in the white matter of Control, Large WMS, and Large WMS + Small WMS cohorts at the 3-month timepoint. Each section was analyzed separately. **(B)** Quantification of NF160 intensity in the white matter. n= 5; **P<0.01: Control vs Large WMS + Small WMS, ****P<0.0001: Control vs Large WMS + Small WMS, $$$P<0.001: Control vs Large WMS, $$$$P<0.0001: Control vs Large WMS, Two-way ANOVA was conducted via Tukey's multiple comparisons test; values are mean with standard error mean (SEM).

Figure 9: Less MBP intensity in the white matter of Large WMS and Large WMS + Small WMS cohorts when compared to Control.

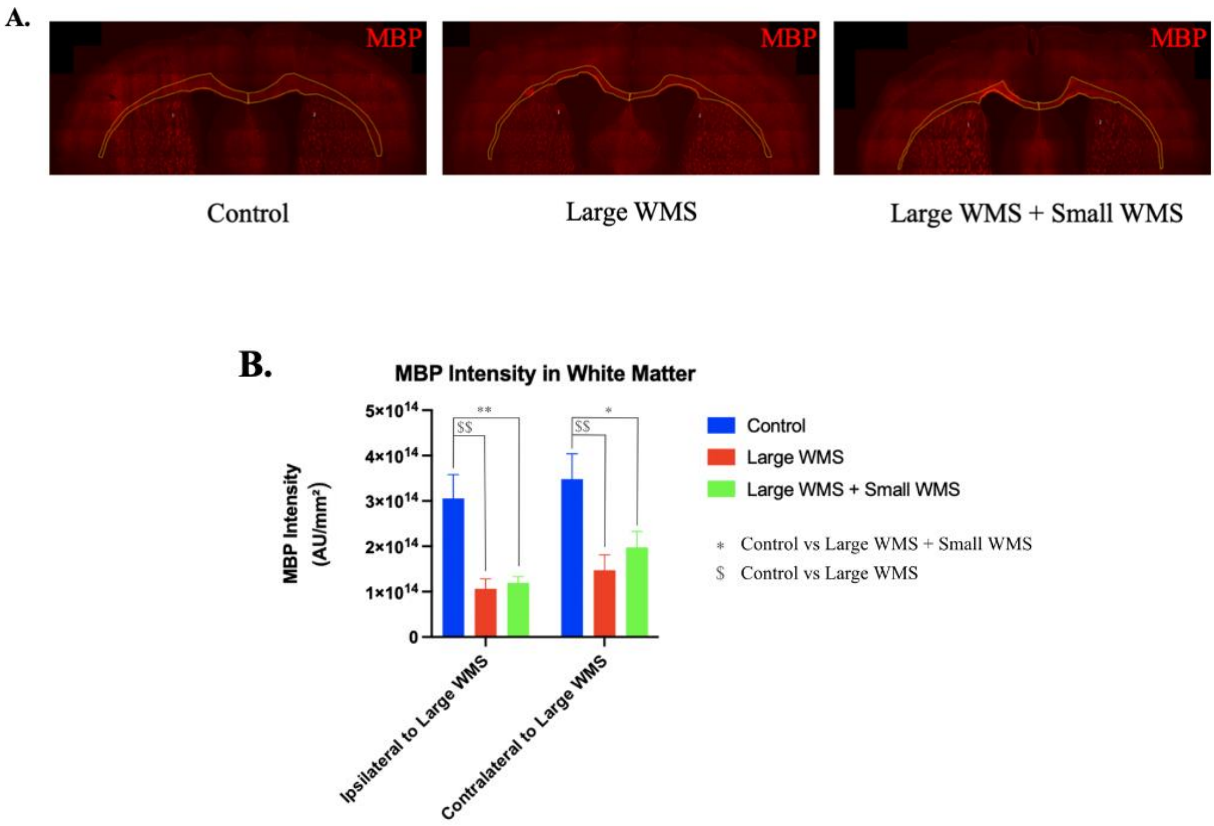

Figure 9: **(A)** Sections were stained with MBP for intensity quantification in the white matter of Control, Large WMS, and Large WMS + Small WMS cohorts at the 3-month timepoint. **(B)** Quantification of MBP intensity in the white matter. n= 5; *P<0.05: Control vs Large WMS + Small WMS, **P<0.01: Control vs Large WMS + Small WMS, $$P<0.01: Control vs Large WMS, Two-way ANOVA was conducted via Tukey's multiple comparisons test; values are mean with standard error mean (SEM).

Figure 10: GFAP intensity in the white matter of Large WMS cohort significantly less when compared to Control.

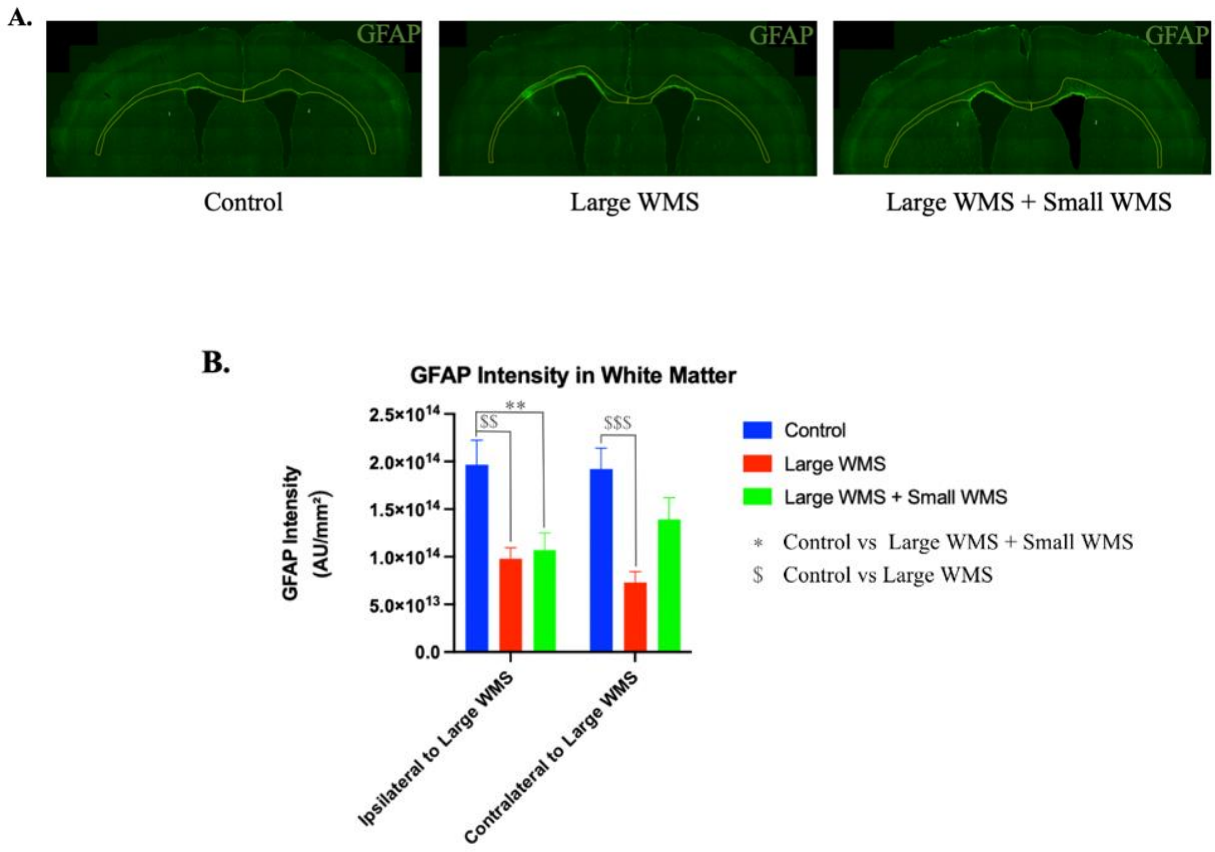

Figure 10: **(A)** Sections were stained with GFAP for intensity quantification in the white matter of Control, Large WMS, and Large WMS + Small WMS cohorts at the 3-month timepoint. **(B)** Quantification of GFAP intensity in white matter. n= 5; **P<0.01: Control vs Large WMS + Small WMS, $$P<0.01: Control vs Large WMS, $$$P<0.001: Control vs Large WMS, Two-way ANOVA was conducted via Tukey's multiple comparisons test; values are mean with standard error mean (SEM).

References

1. Antunes, M., and G. Biala. “The novel object recognition memory: Neurobiology, test procedure, and its modifications.” *Cognitive Processing*, vol. 13, no. 2, 9 Dec. 2011, pp. 93–110, https://doi.org/10.1007/s10339-011-0430-z.
2. Carmichael, S. Thomas, and Irene L. Llorente. “The ties that bind: Glial transplantation in white matter ischemia and vascular dementia.” *Neurotherapeutics*, vol. 20, no. 1, Jan. 2023, pp. 39–47, https://doi.org/10.1007/s13311-022-01322-8.
3. “How Many People Are Affected by/at Risk for Stroke?” *Eunice Kennedy Shriver National Institute of Child Health and Human Development*, U.S. Department of Health and Human Services, 1 Feb. 2022.
4. Iadecola, Costantino. “The pathobiology of vascular dementia.” *Neuron*, vol. 80, no. 4, Nov. 2013, pp. 844–866, https://doi.org/10.1016/j.neuron.2013.10.008.
5. Kalaria, Raj N., et al. “Stroke injury, cognitive impairment and vascular dementia.” *Biochimica et Biophysica Acta (BBA) - Molecular Basis of Disease*, vol. 1862, no. 5, May 2016, pp. 915–925, https://doi.org/10.1016/j.bbadis.2016.01.015.
6. Kuriakose, Diji, and Zhicheng Xiao. “Pathophysiology and treatment of stroke: Present status and future perspectives.” *International Journal of Molecular Sciences*, vol. 21, no. 20, 15 Oct. 2020, pp. 1–24, https://doi.org/10.3390/ijms21207609.
7. Llorente, Irene L., et al. “Patient-derived glial enriched progenitors repair functional deficits due to white matter stroke and vascular dementia in rodents.” *Science Translational Medicine*, vol. 13, no. 590, 21 Apr. 2021, pp. 1–17, https://doi.org/10.1126/scitranslmed.aaz6747.

8. Mackenzie, Ruairi J. “Gray Matter vs White Matter.” *Neuroscience from Technology Networks*, 20 Aug. 2019.

9. Marin, Miguel Alejandro, and S. Thomas Carmichael. “Stroke in CNS white matter: Models and Mechanisms.” *Neuroscience Letters*, vol. 684, Sept. 2018, pp. 193–199, https://doi.org/10.1016/j.neulet.2018.07.039.

10. Matute, Carlos, et al. “Protecting white matter from stroke injury.” *Stroke*, vol. 44, no. 4, Apr. 2013, pp. 1204–1211, https://doi.org/10.1161/strokeaha.112.658328.

11. O’Brien, John T, and Alan Thomas. “Vascular dementia.” *The Lancet*, vol. 386, no.10004, Oct. 2015, pp. 1698–1706, https://doi.org/10.1016/s0140-6736(15)00463-8.

12. Robertson, Sally. “What Is Grey Matter?” *News Medical Life Sciences*, 10 June 2023.

13. Rosenzweig, Shira, and S. Thomas Carmichael. “Age-dependent exacerbation of white matter stroke outcomes.” *Stroke*, vol. 44, no. 9, Sept. 2013, pp. 2579–2586, https://doi.org/10.1161/strokeaha.113.001796.

14. Ruan, Jingsong, and Yao Yao. “Behavioral tests in rodent models of stroke.” *Brain Hemorrhages*, vol. 1, no. 4, Dec. 2020, pp. 171–184, https://doi.org/10.1016/j.hest.2020.09.001.

15. Shoji, Hirotaka, et al. “Contextual and cued fear conditioning test using a video analyzing system in mice.” *Journal of Visualized Experiments*, no. 85, 1 Mar. 2014, pp. 1–13, https://doi.org/10.3791/50871.

16. Sozmen, Elif G., et al. “A white matter stroke model in the mouse: Axonal damage, progenitor responses and MRI correlates.” *Journal of Neuroscience Methods*, vol. 180, no. 2, June 2009, pp. 261–272, https://doi.org/10.1016/j.jneumeth.2009.03.017.

17. Sozmen, Elif G., Jason D. Hinman, et al. “Models that matter: White matter stroke models.” *Neurotherapeutics*, vol. 9, no. 2, Apr. 2012, pp. 349–358, https://doi.org/10.1007/s13311-012-0106-0.

18. Syeara, Nausheen, et al. “The finer aspects of grid-walking and cylinder tests for experimental stroke recovery studies in mice.” *Methods in Molecular Biology*, vol. 2616, 2023, pp. 345–353, https://doi.org/10.1007/978-1-0716-2926-0_23.

19. “Treat and Recover from Stroke.” *Centers for Disease Control and Prevention*, Centers for Disease Control and Prevention, 4 May 2023.

20. Unnithan, Ajaya Kumar A., et al. *Hemorrhagic Stroke*. StatPearls.

21. Walhovd, K.B., et al. “Unraveling the secrets of white matter – bridging the gap between cellular, Animal and Human Imaging Studies.” *Neuroscience*, vol. 276, Sept. 2014, pp. 2–13, https://doi.org/10.1016/j.neuroscience.2014.06.058.

22. Wang, Yuan, et al. “White matter injury in ischemic stroke.” *Progress in Neurobiology*, vol. 141, June 2016, pp. 45–60, https://doi.org/10.1016/j.pneurobio.2016.04.005.

23. Wen, Quan, and Dmitri B Chklovskii. “Segregation of the brain into gray and white matter: A design minimizing conduction delays.” *PLoS Computational Biology*, vol. 1, no. 7, 30 Dec. 2005, pp. 0617–0630, https://doi.org/10.1371/journal.pcbi.0010078.

24. Zeiler, Steven R., et al. “Paradoxical motor recovery from a first stroke after induction of a second stroke.” *Neurorehabilitation and Neural Repair*, vol. 30, no. 8, 10 July 2016, pp. 794–800, https://doi.org/10.1177/1545968315624783.